

# Cation exchange membrane and anion exchange membrane aided electrolysis processes for hypochlorite generation

Seong K. Kim<sup>\*†</sup>, Dong-Min Shin<sup>†</sup> and Ji Won Rhim<sup>\*\*†</sup>

Department of Chemical Engineering, Hannam University, 1646 Yuseongdae-ro, Yuseong-gu, Daejeon, 34054, Republic of Korea

(Received July 3, 2021, Revised February 15, 2023, Accepted March 7, 2023)

**Abstract.** In this study, the influence of different IEMs (ion exchange membranes) to performance of the hypochlorite electrolysis unit with Cl<sub>2</sub> recovery stream was investigated. More specifically, Nafion 117—a representative cation exchange membrane (CEM)—and aminated polyphethylene oxide (APPO)—an anion exchange membrane (AEM)—were installed in the hypochlorite electrolysis unit, and the performance and the energy efficiency of the units were evaluated and compared. Regardless of whether CEM (Nafion 117) or AEM (APPO) was installed, the rate of hypochlorite generation was increased (by up to 24.3% and 22.2% for Nafion 117 and APPO, respectively) compared with the unit without an IEM. On the other hand, the power efficiency and the optimum operation condition of hypochlorite production units seem to depend on the conductivity and stability of the installed IEM. As the result, between Nafion 117 and APPO, higher performance and efficiency were achieved with Nafion 117, due to excellent conductivity and stability of the membrane.

**Keywords:** APPO; electrolysis; hypochlorite; ion exchange membrane; Nafion; virus removal

## 1. Introduction

Hypochlorous acid and other hypochlorites (e.g. sodium hypochlorite, potassium hypochlorite, etc.) are utilized frequently as disinfectants and cleaning agents (Severing *et al.* 2019, Lantagne 2008, Lu *et al.* 2021). The outstanding disinfecting ability of the hypochlorous acid (HOCl) and sodium hypochlorite (NaOCl) are already well-known (Mara and Horan 2003, Wilhelm *et al.* 2008), and these hypochlorites have been frequently utilized to disinfect wastewater at wastewater treatment plants (Zierof *et al.* 1998, Twort *et al.* 2000, Vijayaraghavan *et al.* 1999). However, when utilizing hypochlorites in wastewater treatment plants, safely storing sodium hypochlorite in bulk amount can become a challenge, since sodium hypochlorite easily decomposes into chlorine gas in atmospheric condition, thus, can be hazardous to the worker's health and surrounding environment (Piskin and Turkun 1995, Urban 2007, Bommaraju 1995). For this reason, *in-situ* electrolysis of NaOCl is considered as the effective and safe method to generate hypochlorites on-site for disinfection of wastewater (Vijayaraghavan *et al.* 1999). In addition, the method can be considered cost-efficient since generation of hypochlorites *via* electrolysis only require brine (sodium chloride solution) and small amount of electricity (Vijayaraghavan *et al.* 2008, Kim *et al.* 2021).

Despite the advantages that the hypochlorites electrolysis

process can offer, development of *in-situ* wastewater disinfecting units still requires further research because the current electrolysis cells present some issues related to production efficiency, controllability, stability during operation, and generation of harmful by-products (Jung *et al.* 2010, Wang *et al.* 2020). As a method to overcome these issues, an ion exchange membrane (IEM) may be installed in the electrolysis cell (Lee *et al.* 2018). After installation of an IEM, the electrolysis cell would be divided into two chambers: a cathodic chamber (at which the cathodic reaction occur) and an anodic chamber (where the anodic reaction occur) (Kim *et al.* 2015, 2021). With the IEM physically dividing the two chambers, the environment in which the cathodic reaction and the anodic reaction occur can be controlled separately. For example, it is possible to maintain the anodic chamber at low pH, while keeping the cathodic chamber (and the cathodic reaction) at high pH, thus, affecting the kinetics of hypochlorite generation. Depending on the IEM used, it is also possible to selectively transport cations or anions between the chambers, which may also become a factor that affects the hypochlorite electrolysis. For example, CEMs (e.g. Nafion and SPEEK) selectively transport cations, such as proton and sodium ions, between two chambers of the electrolysis cell. Contrarily, AEMs (e.g. APPO) selectively transport anions such as hydronium (OH<sup>-</sup>) and chlorine ions (Cl<sup>-</sup>). In addition to inserting an IEM to the electrolysis cell, installing a chlorine (Cl<sub>2</sub>) recovery stream can help increasing the performance of the hypochlorite generation process, especially if an excess amount of chlorine gas is formed during electrolysis (Kim *et al.* 2021, Sanchez-Aldana *et al.* 2018). Furthermore, the kinetics of formation of byproducts, such as chlorates and perchlorates, are known to depend strongly on electrolysis conditions such as

\*Corresponding author, Professor,  
E-mail: starkme@hnu.kr

\*\*Co-corresponding author, Professor,  
E-mail: jwrhim@hnu.kr

† These authors contributed equally to this work

pH (Levanov and Isaikina 2020, Gordon and Tachiyashiki 1991), and pH controlled environment made with insertion of the IEM can effectively decrease the byproduct formation (Jung *et al.* 2010).

In this study, the influence of the selective ion transport to an in-situ hypochlorite electrolysis of brine with  $\text{Cl}_2$  recovery stream was investigated. By inserting Nafion 117 as a representative CEM and APPO as an AEM, the selective ion transport between the anode and the cathode of the electrolysis cell was achieved, which consequently enhanced the hypochlorite generation rate and efficiency of the electrolysis cell. For further investigation, the ion conductivities of Nafion 117 and APPO membranes saturated in NaCl solution was measured, and then the rates of hypochlorite generation of the electrolysis cell with and without IEMs before and after installation of  $\text{Cl}_2$  recovery stream were compared. Notably, the performance of the hypochlorite generation system enhanced when either IEM was installed in the electrolysis cell if  $\text{Cl}_2$  recovery stream was present, which indicates both CEM and AEM can effectively induce the hypochlorite generation with aid of  $\text{Cl}_2$  recovery.

## 2. Experimental methods

### 2.1 Materials

As IEMs installed in the electrolysis cell, Nafion 117 membranes purchased from Chemours and APPO membranes provided by Siontech (Republic of Korea) were used as CEM and AEM, respectively. For electrolysis experiments, 200 g  $\text{L}^{-1}$  brine solution produced with ultra-pure deionized water generated using AquaMax™ Water Purification System (Younglin Instrument, Korea) and sodium chloride (Samchun Chemicals, Korea) was used.

### 2.2 Membrane characterizations and ion conductivity measurements

For characterization of Nafion 117 membranes and APPO membranes, Fourier transform infrared spectroscopy (FT-IR, Alpha-P; Bruker) in attenuated total reflectance (ATR) mode was utilized. The IR spectra were obtained at wavenumbers between 400  $\text{cm}^{-1}$  and 4000  $\text{cm}^{-1}$  with scan rate of 4  $\text{cm}^{-1} \text{ s}^{-1}$ .

Ion conductivities of the membranes were measured using an electrochemical workstation (Zive MP1 Multi-channel Workstation; Zive Lab) *via* ac-impedance spectroscopy. All ac-impedance spectroscopy measurements were conducted from 1 MHz to 100 mHz with applied ac-potential of 50 mV. The measurements were performed at room temperature under two different conditions: after submerging in deionized water for more than 12 h (similar to 100% RH condition) and after fully saturating under 200 g  $\text{L}^{-1}$  NaCl solution.

### 2.3 Hypochlorite generation

Hypochlorites were generated through electrolysis

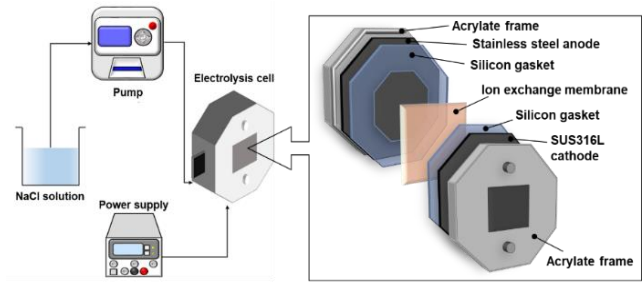


Fig. 1 Schematic description of the electrolysis cell for hypochlorite generation

process with  $\text{Cl}_2$  recovery stream. The detailed schematic of the electrolysis cell is shown in Fig. 1.

The electrolysis cell consists of a stainless steel based Dimensionally Stable Anode (DSA) provided by Techwin (South Korea) as the anode, and SUS316L mesh purchased from ATX as the cathode. The anode and cathode were set-up in the electrolysis cell with 0.4 cm between the electrodes, and the IEM was installed at the middle. The brine solution was fed into the electrolysis cell at concentration of 200 g  $\text{L}^{-1}$  with flow rate of 50  $\text{mL min}^{-1}$ . The flow rate of the inlet was controlled using a Model 7519-06 mechanical pump from Masterflex. For electrolysis process, the electric currents were supplied at 100, 200, 300, and 400  $\text{mA cm}^{-1}$  using a power supply. As the result of the electrolysis process, chlorine gas ( $\text{Cl}_2$ ), hypochlorous acid ( $\text{HOCl}$ ), and sodium hypochlorite ( $\text{NaOCl}$ ) were generated. The excess chlorine gas was collected in vapor phase and bubbled through the outflow from the cathodic chamber. The product stream of the hypochlorite generation system was collected for 100 mins. The concentration of the product stream was measured by titration. The titration was performed using 0.2 M sodium thiosulfate ( $\text{Na}_2\text{S}_2\text{O}_3$ ) solution with the mixture of potassium iodide, acetic acid, and aqueous starch solution as the indicator. The total amount of  $\text{HOCl}$  and  $\text{NaOCl}$  produced and concentration of the hypochlorite ions in the product stream were calculated using Equation 1 and 2, respectively:

$$\begin{aligned} \text{mmoles of Hypochlorites (mmol)} \\ = V_{\text{Na}_2\text{S}_2\text{O}_3} (\text{mL}) \times 0.1 \end{aligned} \quad (1)$$

$$\begin{aligned} \text{Conc. Hypochlorites (mM)} \\ = \frac{\text{mmoles of Hypochlorites (mmol)}}{V_{\text{sample}} (\text{L})} \end{aligned} \quad (2)$$

where  $V_{\text{Na}_2\text{S}_2\text{O}_3}$  is the volume of 0.2 M  $\text{Na}_2\text{S}_2\text{O}_3$  used for titration in mL and  $V_{\text{sample}}$  is the volume of the product used for titration in liter (Wilson 1935).

## 3. Results and discussion

### 3.1 Description of the designed process

The effect of different IEMs to the hypochlorite electrolysis process with  $\text{Cl}_2$  recovery stream (Fig. 2) was investigated in this study.

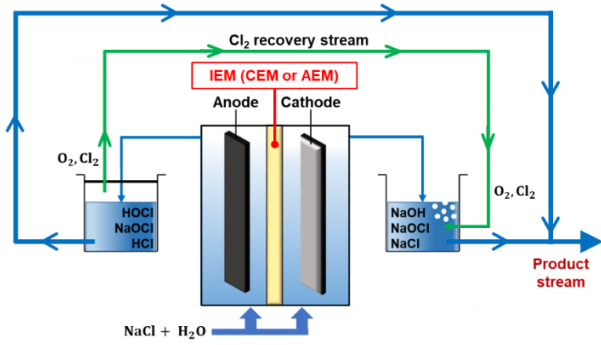


Fig. 2 Schematic flow diagram of the hypochlorite electrolysis system with  $\text{Cl}_2$  recovery stream

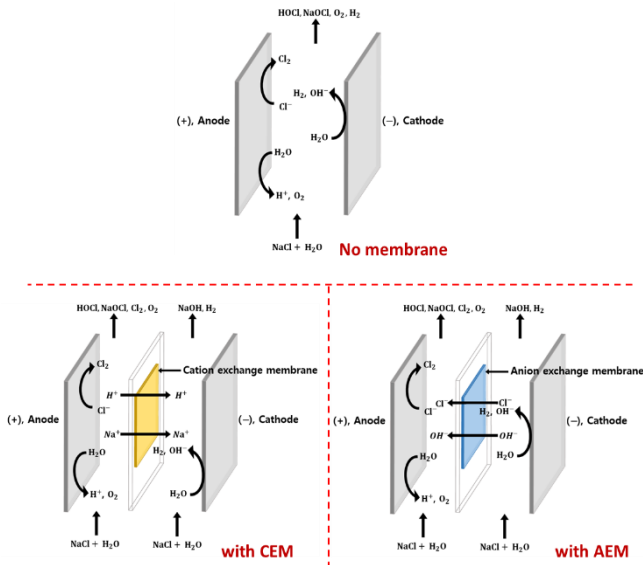
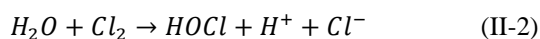
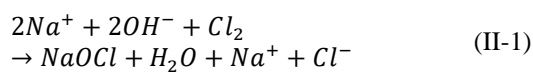
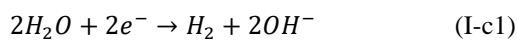
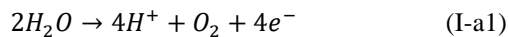


Fig. 3 Schematics describing the electrolysis reactions that occur without IEM (top), with CEM (bottom left), and with AEM (bottom right)

As described in Fig. 2, the brine solution was fed into the electrolysis cell with or without an IEM. When an IEM is installed, the electrolysis cell is physically divided into two chambers: the anodic chamber at which oxidation of  $\text{Cl}^-$  ion occur, and the cathodic chamber where  $\text{H}_2\text{O}$  molecules reduces to form  $\text{OH}^-$  ions. Without a membrane, the electrolysis process follows a two-step reaction.



The first step involves oxidation of hydrogen in water molecules (I-a1) and  $\text{Cl}^-$  ions (I-a2) to form  $\text{H}^+$  ions, oxygen

gas ( $\text{O}_2$ ), and  $\text{Cl}_2$  at the surface of anode of the electrolysis unit, and reduction of hydrogen in water molecules (I-c1) to form hydrogen gas ( $\text{H}_2$ ) and hydronium ions ( $\text{OH}^-$ ) at the surface of the cathode. The Reaction Step I is closely followed by the Reaction Step II, which consists of formation of  $\text{NaOCl}$  (II-1) and  $\text{HOCl}$  (II-2) from spontaneous reactions between  $\text{Cl}_2$  molecules and  $\text{NaOH}$  or  $\text{H}_2\text{O}$ . In the  $\text{Cl}_2$  recovery stream,  $\text{O}_2$  is also present, but an additional separation process was not necessary because of  $\sim 3$  orders of magnitude lower solubility of  $\text{O}_2$  in water at ambient condition. From reaction II-1 and II-2, we can easily suspect that formation of  $\text{NaOCl}$ , which involves  $\text{OH}^-$  as a reactant, is favored at a basic environment, while formation of  $\text{HOCl}$  would be favored at a relatively acidic environment. As expected, it is reported in previous studies that the formation of  $\text{NaOCl}$  is highly favored at pH above 9, and  $\text{HOCl}$  is favored at pH below 6 (Kim *et al.* 2021, Ryu *et al.* 2018).

Consequently, formation of  $\text{NaOCl}$  would be greatly suppressed after installation of a CEM (middle of Fig. 3). Due to the physical separation created by the installed CEM,  $\text{OH}^-$  ions formed *via* Reaction I-C1 cannot gain access to  $\text{Cl}_2$  molecules, which are formed at the surface of anode; thus,  $\text{NaOCl}$  formation is disfavored. Simultaneously, because of the physical division, the anodic chamber of the electrolysis cell is maintained at an acidic condition (typically pH  $\sim 3$ ) during operation. For these reasons, formation of  $\text{HOCl}$  is enhanced for the electrolysis unit installed with CEM, while excess amount of unreacted  $\text{Cl}_2$  is also generated (due to suppressed Reaction I-C1). However, the unreacted  $\text{Cl}_2$  can easily be collected in vapor phase, which can be bubbled through the outlet stream of the cathodic chamber at pH  $\sim 10$  to further generate  $\text{NaOCl}$ . Similarly, when AEM is installed in the electrolysis cell (right of Fig. 3), the anode and cathode of the electrolysis cell is physically divided. However, unlike the case of CEM,  $\text{OH}^-$  is transferred from the cathodic chamber to the anodic chamber; thus, the pH difference between two chambers can be mediated. The effect of the pH mediation can depend on the anion conductivity of the membrane, applied electric field to the membrane, and the gradient of the  $\text{OH}^-$  concentration between two chambers. Theoretically, the mediated pH difference between two chambers can influence the performance of the hypochlorite generation unit. In this study, the effects of installed CEM and AEM to the performance of the hypochlorites electrolysis unit are investigated using Nafion 117, a representative cation exchange membrane, and aminated polyphenylene oxide (APPO), which is an anion exchange membrane.

### 3.2 Characterization and properties of Nafion 117 and APPO membranes

The results of the Fourier transform infrared spectroscopy (FT-IR) and the chemical structure of the Nafion 117 and APPO membranes are shown in Fig. 4 and Fig. 5.

Fig. 4 consists of the IR spectrum obtained for Nafion 117 with its chemical structure in the inset. In Fig. 4, a

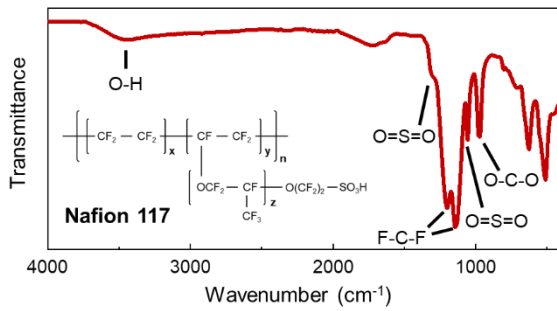


Fig. 4 IR spectrum obtained from Nafion 117 membrane

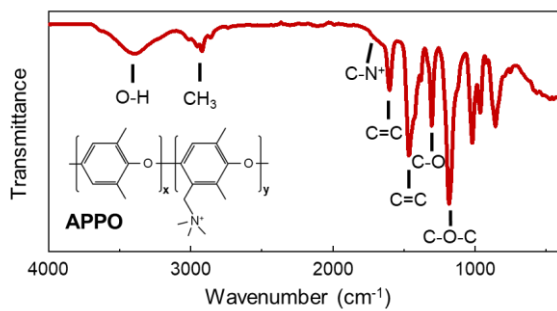


Fig. 5 IR spectrum obtained from APPO membrane

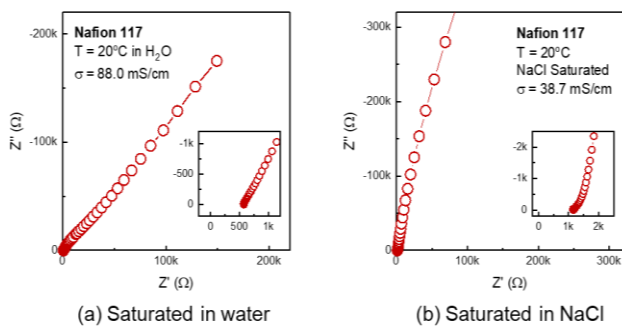


Fig. 6 Nyquist plots obtained for Nafion 117 membrane after saturating in (a) deionized water and (b) NaCl solution

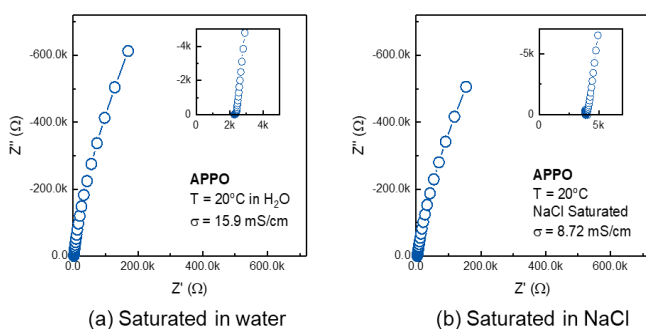


Fig. 7 Nyquist plots obtained for APPO membrane after saturating in (a) deionized water and (b) NaCl solution

broad peak corresponding to stretching of O-H bonds near  $3440\text{ cm}^{-1}$ , peaks related to asymmetric and symmetric stretching of S=O bonds near  $1310\text{ cm}^{-1}$  and  $1050\text{ cm}^{-1}$ , respectively, peaks corresponding to stretching and bending

of C-F bonds at  $1210\text{ cm}^{-1}$  and  $1140\text{ cm}^{-1}$ , and a peak from stretching of C-O-C at  $975\text{ cm}^{-1}$  were observed. This spectrum is similar to the previously reported IR spectra of Nafion 117 membranes (Ryu *et al.* 2018). The IR spectrum of APPO is shown in Fig. 5, from which an IR spectrum similar to polyphenylene oxide (PPO) was observed. Similar to the reported IR spectrum of PPO, a broad peak corresponding to stretching of O-H near  $3400\text{ cm}^{-1}$ , a set of peaks related to stretching of C-H bonds near  $2930\text{ cm}^{-1}$ , peaks corresponding to stretching of C=C bonds at  $1610\text{ cm}^{-1}$  and  $1465\text{ cm}^{-1}$ , and peaks corresponding to stretching of C-O bonds near  $1305\text{ cm}^{-1}$  and  $1180\text{ cm}^{-1}$  were observed (Hari Gopi *et al.* 2014). However, in contrast to the IR spectrum of PPO, an additional small peak corresponding to stretching of C-N<sup>+</sup> was observed at  $1690\text{ cm}^{-1}$  from Fig. 5, which confirms the existence of the anion conducting functional group (C-N<sup>+</sup>) of APPO membranes (Arges *et al.* 2015).

The ion conductivities of Nafion 117 and APPO were measured using ac-impedance spectroscopy, and the results were plotted in Nyquist fashion as shown in Fig. 6 and Fig. 7, respectively. The measurement was performed using a membrane conductivity cell (MCC). The results can also be plotted as Bode plots (Fig. 8) as well, which shows the frequency dependent impedance and phase angle.

Fig. 6a and 6b consist of Nyquist plots obtained from the impedance measurement of Nafion 117 after saturation under deionized water and NaCl solution at room temperature. When saturated under deionized water, only proton conducts through Nafion 117; thus, the conductivity ( $88.0\text{ mS cm}^{-1}$ ) observed is mainly from conduction of proton through Nafion 117. The measured proton conductivity of Nafion 117 is similar to previously reported values (Ryu *et al.* 2018, Ko *et al.* 2018, Sone *et al.* 1996). After saturating with the brine solution, both proton and sodium ion (Na<sup>+</sup>) transfer through the membrane. Since Na<sup>+</sup> ions are heavier compared to proton, the effective mobility of Na<sup>+</sup> ion would be smaller; therefore, the conductivity of the Nafion 117 membrane was decreased to  $38.7\text{ mS cm}^{-1}$ . As the evidence of the difference in effective mobility, the characteristic frequency of Nafion 117 saturated with NaCl (Fig. 8b) was smaller than Nafion 117 saturated with deionized water (Fig. 8a). Similar trend can be observed from APPO membrane. When hydrated with deionized water, the APPO membrane (as an AEM) conducts OH<sup>-</sup> ions, while APPO saturated in the brine solution would transfer both OH<sup>-</sup> and Cl<sup>-</sup> ions (Palaty and Bendova 2010). Thus, the ion conductivity decreased from  $15.9\text{ mS cm}^{-1}$  to  $8.72\text{ mS cm}^{-1}$  upon introduction of NaCl (Fig. 7). However, even though decrease in conductivities were observed, the decreases are less than an order of magnitude. Likewise, similar characteristic frequencies were observed for H<sub>2</sub>O and NaCl saturated APPO, which can be explained by similar effective mass between OH<sup>-</sup> ions and Cl<sup>-</sup> ions (Fig. 8c and 8d). For both CEM and AEM installed electrolysis cell, if the conductivity of the membrane is high enough, the difference in pH between two chambers of the cell would be mediated. To investigate the influence of these membranes, the electrolysis processes aided by CEM and AEM need to be studied in more detail.

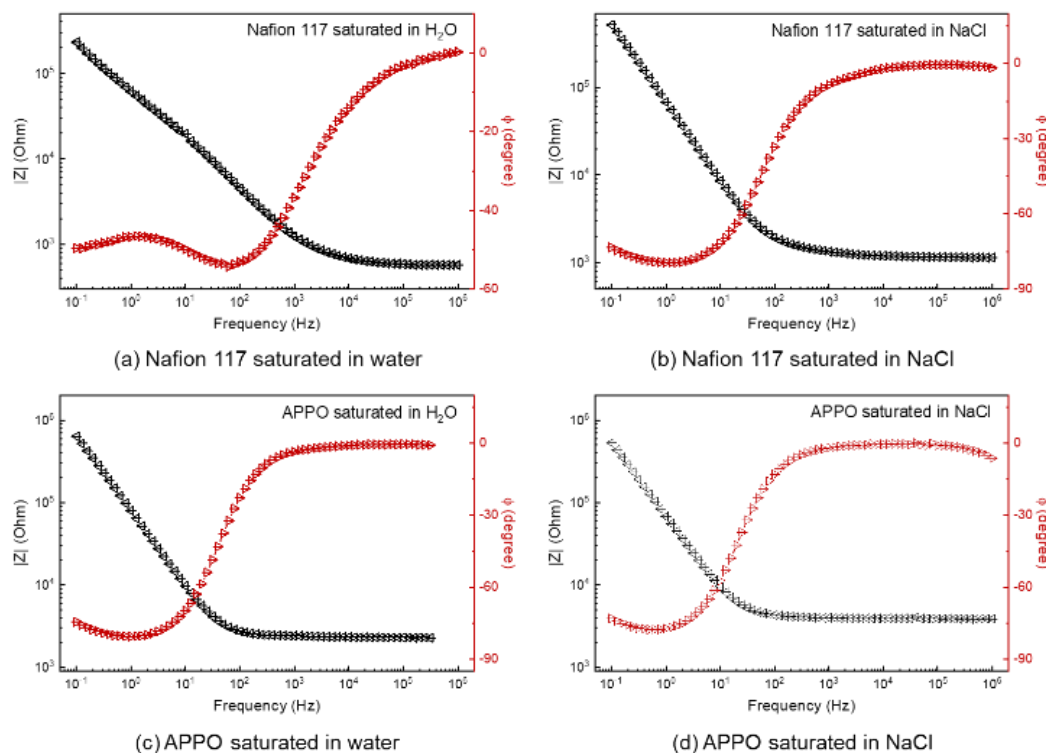


Fig. 8 Frequency dependent impedance plots for Nafion 117 and APPO saturated in (a, c) deionized water and (b, d) NaCl solution, respectively

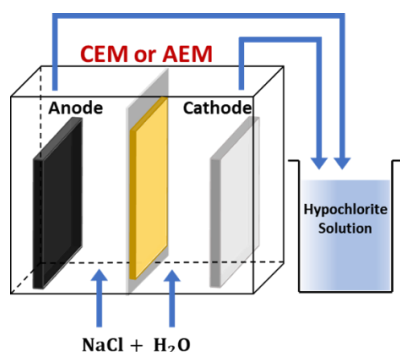


Fig. 9 Schematic of the experiment performed to evaluate the performance of the hypochlorite electrolysis process only

### 3.3 Hypochlorite electrolysis with Nafion 117 and APPO (without $\text{Cl}_2$ recovery)

To compare and understand the effect of the different IEM installed in the electrolysis cell for hypochlorite generation, the outputs of the electrolysis cells without the  $\text{Cl}_2$  recovery stream were investigated first (Fig. 9). Fig. 10a-c include the concentration of hypochlorites and the rate of hypochlorite generation resulted from electrolysis of  $200 \text{ g L}^{-1}$  brine solution without IEM (denoted as No Membrane), with Nafion 117 membrane, and with APPO membrane at different electric currents. As apparent from the comparable hypochlorite concentrations and rates of production, the amount of hypochlorites generated from the electrolysis cells with Nafion 117 and APPO were similar to that of No Membrane at current densities below  $300 \text{ mA cm}^{-1}$  even with absence of  $\text{Cl}_2$  recovery stream. On the other

hand, the performance of the No Membrane cell was better than those of electrolysis cells with Nafion 117 and APPO when operated at  $400 \text{ mA cm}^{-1}$ . At  $400 \text{ mA cm}^{-1}$ , the hypochlorite electrolysis cell without IEM generated  $2.011 \text{ mol m}^{-2} \text{ min}^{-1}$  at concentration of  $73.0 \text{ mM}$ , while electrolysis cells with Nafion 117 and APPO generated  $1.625$  and  $1.598 \text{ mol m}^{-2} \text{ min}^{-1}$  at  $59.0$  and  $58.0 \text{ mM}$ , respectively.

### 3.4 Hypochlorite electrolysis with Nafion 117 and APPO (with $\text{Cl}_2$ recovery)

During the hypochlorites electrolysis process,  $\text{Cl}_2$  molecules are generated as the intermediate products, which remain unreacted depending on the condition at which the electrolysis was performed. When the unreacted  $\text{Cl}_2$  is bubbled through a solution containing  $\text{NaOH}$ ,  $\text{NaOCl}$  can be generated spontaneously. During the experiment, it was clear that almost all  $\text{Cl}_2$  molecules were reacted to form  $\text{NaOCl}$  via bubbling through  $\text{NaOH}$  solution since distinct odor of the  $\text{Cl}_2$  gas could not be sensed any more. The amounts (in mmol) of hypochlorites generated via each step of the hypochlorite generation process are included in Fig. 11b and 11c. By electrolysis, significant amount of hypochlorites between  $50$  and  $220 \text{ mmol}$  during  $100$  mins of operation. The amount of hypochlorite generated depended on the electric current applied, while the difference in hypochlorite generation among electrolysis cells without an IEM, with Nafion 117, with APPO was not too significant when considering only the electrolysis process without  $\text{Cl}_2$  recovery. Contrarily, the amount of hypochlorites generated from the  $\text{Cl}_2$  recovery stream for

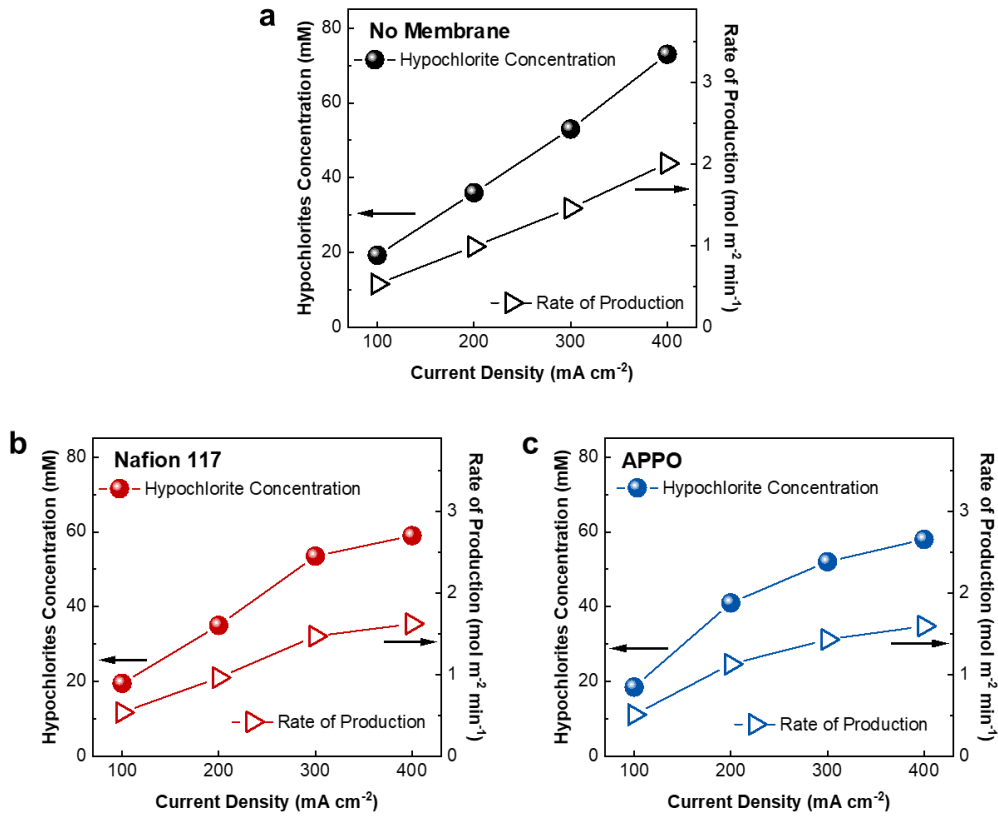


Fig. 10 Hypochlorite concentration and rate of hypochlorite production by (a) electrolysis cell without an IEM compared with (b) CEM (Nafion 117) installed electrolysis cell and (c) AEM (APPO) installed electrolysis cell

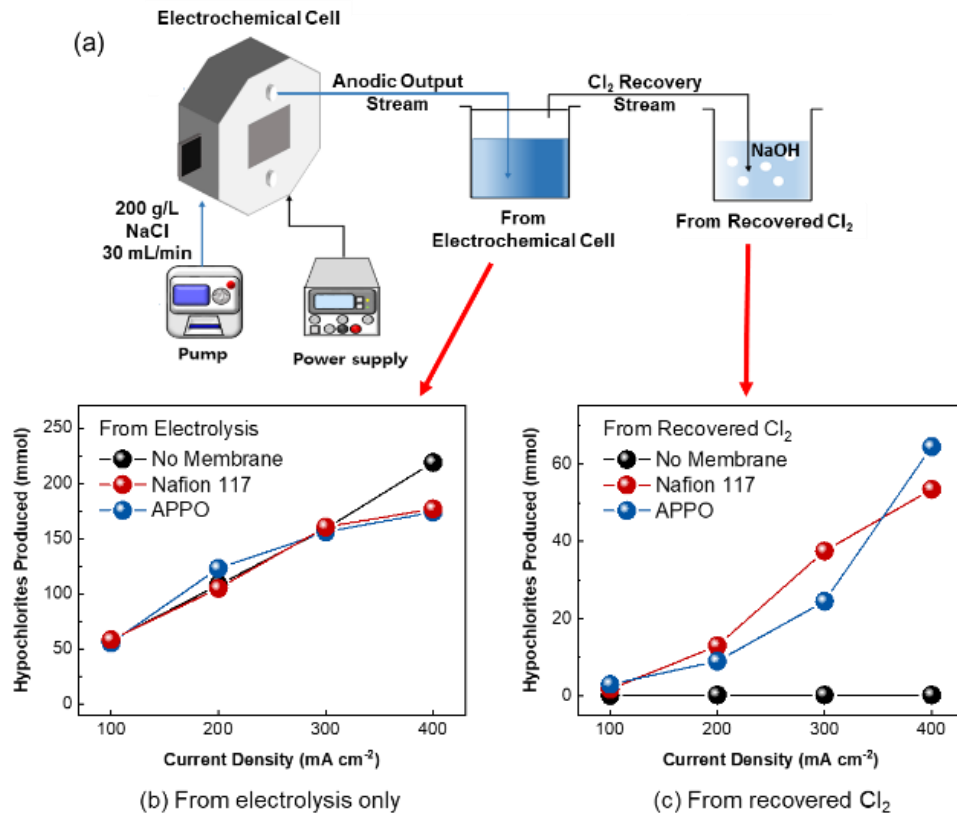


Fig. 11 Amount of hypochlorite generated by the electrolysis cells with Cl<sub>2</sub> recovery stream. (a) Process diagram of the hypochlorite generation system and amounts of hypochlorite generated from (b) the electrolysis process only vs. (c) *via* recovered Cl<sub>2</sub>

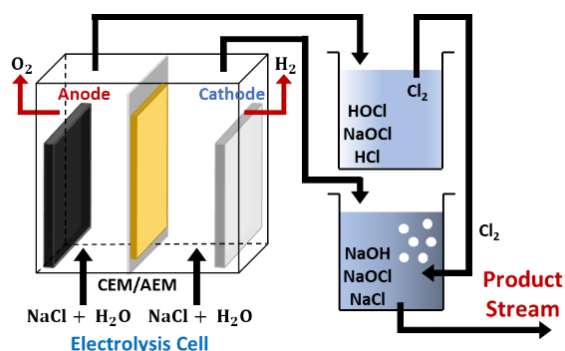


Fig. 12 Schematic description of the proposed IEM added hypochlorite generation system with  $\text{Cl}_2$  recovery stream

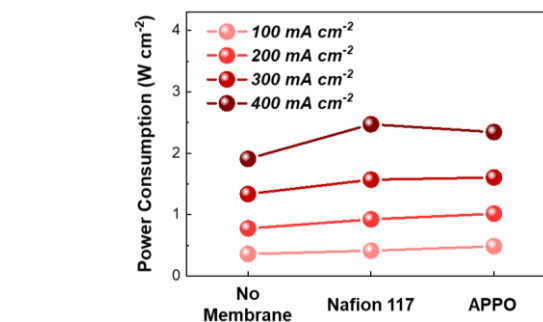
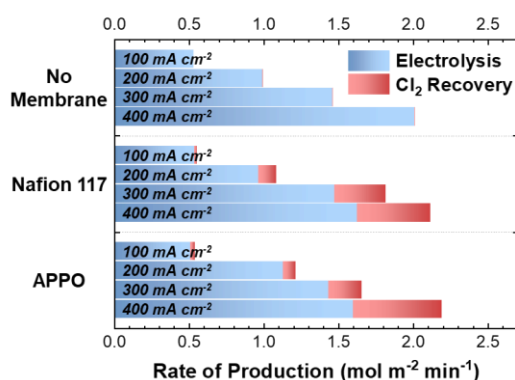


Fig. 14 Electric power consumed during hypochlorite generation for systems with No Membrane, Nafion 117, and APPO

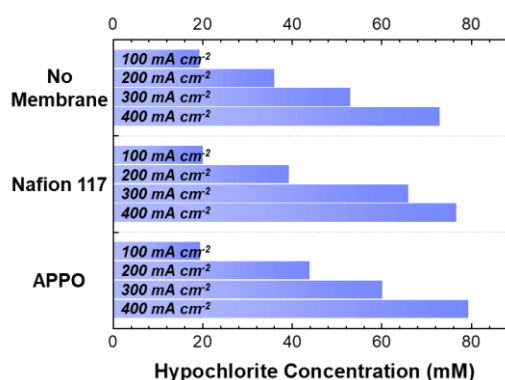


Fig. 13 Rate of production (left), concentration of hypochlorite (right) measured at the product stream

No Membrane case was negligible small (less than 10 mmol), while considerable amounts of hypochlorites were generated from the  $\text{Cl}_2$  recovery streams of electrolysis cells with Nafion 117 and with APPO. In fact, a negligibly small amount of  $\text{Cl}_2$  molecules seemed to form when the electrolysis was performed without an IEM in the first place for all applied electric currents; thus, such a result is expected. On the other hand, significant amounts of  $\text{Cl}_2$  molecules remained unreacted probably due to low pH (typically less than 4) in the anodic chamber, which is unfavorable for  $\text{NaOCl}$  generation. The amounts of the unreacted  $\text{Cl}_2$  seemed to depend substantially on the applied electric current as implied by the strong dependence of the hypochlorites generated from the  $\text{Cl}_2$  recovery stream on the applied electric current for both the Nafion 117 and APPO installed cells.

To efficiently utilize the excess  $\text{Cl}_2$  molecules generated in an IEM installed electrolysis cell,  $\text{Cl}_2$  recovered from the anodic chamber of the electrolysis was bubbled through the high pH outflow of the cathodic chamber as shown in Fig. 12. The schematic in Fig. 12 may become a basis for designing a high-performance continuous flow reactor based on IEM aided electrolysis of hypochlorites with  $\text{Cl}_2$  recovery stream. From the process shown in Fig. 12, the rates of hypochlorite production shown in Fig. 13a was acquired. For No Membrane, the total rates of hypochlorite production were 0.532, 0.993, 1.463, and 2.013  $\text{mol m}^{-2} \text{min}^{-1}$  at 100, 200, 300, and 400  $\text{mA cm}^{-2}$ , respectively. At all applied current densities, the total rate of production was almost solely from electrolysis (blue bar). With Nafion 117,

the total rates of production increased to 0.553, 1.084, 1.819, 2.116  $\text{mol m}^{-2} \text{min}^{-1}$  at 100, 200, 300, and 400  $\text{mA cm}^{-2}$ , respectively. The total rates of production also increased (0.537, 1.213, 1.658, and 2.190  $\text{mol m}^{-2} \text{min}^{-1}$  at 100, 200, 300, and 400  $\text{mA cm}^{-2}$ , respectively) with APPO when compared to No Membrane. The increase in the production rates upon installation of the IEMs was possible due to hypochlorites generated from the recovered  $\text{Cl}_2$  (red bar) since considerable portion (up to 28%) of the total rates of hypochlorite production were from the  $\text{Cl}_2$  recovery step (as also shown in Fig. 11). As the result of the addition of IEM and  $\text{Cl}_2$  recovery stream, the rate of hypochlorite generation was enhanced by up to 24.3% for Nafion 117 at 300  $\text{mA cm}^{-2}$  and by up to 22.2% for APPO membranes at 200  $\text{mA cm}^{-2}$ . The observed difference in the optimum current density of operation between two membranes can be useful when designing an actual hypochlorite generation unit. Besides the rate of production, the concentration of hypochlorites in the product stream also increased upon installation of IEMs (Fig. 13b). For the case of No Membrane, the concentrations of the hypochlorites at the product streams were 19.31, 36.08, 53.09, and 73.09 mM respectively at 100, 200, 300, and 400  $\text{mA cm}^{-2}$  of applied current densities. On the other hand, if Nafion 117 was installed to the electrolysis cell, the hypochlorite concentration increased to 20.08, 39.34, 66.01, 76.82 mM at 100, 200, 300, and 400  $\text{mA cm}^{-2}$ , respectively. Similarly, installing APPO increased the hypochlorite concentration to 19.51, 44.02, 60.18, 79.50 mM (also at 100, 200, 300, and 400  $\text{mA cm}^{-2}$ , respectively).

Lastly, the electric power consumed by the hypochlorite generation systems with No Membrane, Nafion 117, and APPO are compared in Fig. 14. Consumed electric powers were calculated using the measured electric potential during operation of the electrolysis cells. For both the system with Nafion 117 and APPO, slight increase in consumption of electric power could be observed; however, the increase is not significantly large. For example, when operated at 300 mA cm<sup>-2</sup>, the power consumed by the electrolysis cell were 1.335, 1.569, and 1.605 W cm<sup>-2</sup> for No Membrane, Nafion 117, and APPO, respectively. The unit W cm<sup>-2</sup> indicates the power consumed by the hypochlorite generation cell with size of 1 cm × 1 cm. When comparing the Nafion 117 and APPO with each other, the amount of power consumed were slightly higher for APPO, while the highest increase in the rate of production was observed for Nafion 117. These results suggest that hypochlorite generation can be performed most efficiently with Nafion 117, a representative cation exchange membrane. For both the Nafion 117 and APPO cells, the physical division between the anodic chamber and cathodic chamber was formed stably in the range of electric potentials that were applied; therefore, we can assume that the pH difference between two chambers were established and well-maintained regardless of the type of membrane installed. Hence, the increased rates of hypochlorite generation and outflow concentration could be achieved with both Nafion 117 and APPO. On the other hand, difference in the energy efficiency of the cells with Nafion 117 and APPO may be explained by the difference in the conductivities of two membranes. Due to low ionic conductivity (or high resistance) of the APPO membrane, the potential drop across the membrane would be relatively high; thus, high electric power loss can be caused by the APPO membrane. Nevertheless, both the CEM and AEM enhanced the performance of the hypochlorite generation system, but the conductivity and stability of the membranes used can influence the production rate, outflow concentration, and energy efficiency of the IEM aided hypochlorite electrolysis systems with Cl<sub>2</sub> recovery stream.

#### 4. Conclusions

Enhanced rate of production and outflow (product stream) concentration of the IEM installed hypochlorite electrolysis process with Cl<sub>2</sub> recovery stream were achieved when either CEM (Nafion 117) or AEM (APPO) was utilized as the IEM. With Nafion 117 (as a CEM), the rate of production of the electrolysis cell with Cl<sub>2</sub> recovery stream increased up to 24.3% at applied current density of 300 mA cm<sup>-2</sup>, while the increase was around 22.2% at 200 mA cm<sup>-2</sup> when APPO was installed as an AEM. Regardless of whether a CEM is installed or an AEM is installed to the electrolysis cell, the performances of the hypochlorite generation systems were increased as long as Cl<sub>2</sub> recovery stream was installed; however, the extent of the performance enhancement and optimum operating condition depended on the conductivity and stability of the IEM used in the system. Similarly, the electric power

consumed by the hypochlorite electrolysis also depended on the performance of IEM, and a slightly higher power consumption could be observed for the electrolysis cell with APPO due to its relatively low ionic conductivity, while more efficient hypochlorite generation was achieved with Nafion 117 due to its high ionic conductivity.

#### Acknowledgments

This work was supported by National Research Foundation (NRF) of Korea through grant funded by the Korea government (MSIT) (grant number: 2020R1G1A1101287). S. K. K. also acknowledges the “Basic project (referring to projects performed with the budget directly contributed by the Government to achieve the purposes of establishment of Government-funded research institute)” established due to cooperation project with/supported by the KOREA RESEARCH INSTITUTE OF CHEMICAL TECHNOLOGY (KRICT).

#### References

- Arges, C.G., Wang, L., Jung, M.S. and Ramani, V. (2015), “Mechanically stable poly(arylene ether) anion exchange membrane prepared from commercially available polymers for alkaline electrochemical devices”, *J. Electrochem. Soc.*, **162**, F686-F693. <https://doi.org/10.1149/2.0361507jes>.
- Bommaraju, T.V. (1995), “Sodium hypochlorites: its application and stability in bleaching”, *Water Qual. Res. J.*, **30**, 339-361. <https://doi.org/10.2166/wqrj.1995.031>.
- Gordon, G. and Tachiyashiki, S. (1991), “Kinetics and mechanism of formation of chlorate ion from the hypochlorous acid/chlorite ion reaction at pH 6-10”, *Environ. Sci. Technol.*, **25**, 468-474. <https://doi.org/10.1021/es00015a014>.
- Hari Gopi, K., Gouse Peera, S., Bhat, S.D., Sridhar, P. and Pitchumani, S. (2014), “Preparation and characterization of quaternary ammonium functionalized poly(2,6-dimethyl-1,4-phenylene oxide) as anion exchange membrane for alkaline polymer electrolyte fuel cells”, *Int. J. Hydrog. Energy*, **39**, 2659-2668. <https://doi.org/10.1016/j.ijhydene.2013.12.009>.
- Jung, Y.J., Baek, K.W., Oh, B.S. and Kang, J.W. (2010), “An investigation of the formation of chlorate and perchlorate during electrolysis using Pt/Ti electrodes: the effects of pH and reactive oxygen species and the results of kinetics studies”, *Water Res.*, **44**, 5345-5355. <https://doi.org/10.1016/j.watres.2010.06.029>.
- Kraft, A., Stadelmann, M., Blaschke, M., Kreysig, D., Sandt, B., Schroder, F. and Rennau, J. (1999), “Electrochemical water disinfection part I: Hypochlorite production from very dilute chloride solutions”, *J. Appl. Electrochem.*, **29**, 859-866. <https://doi.org/10.1023/A:1003650220511>.
- Kim, J.S., Cho, E.H., Rhim, J.W., Park, C.J. and Park, S.G. (2015), “Preparation of bi-polar membranes and their application to hypochlorite production”, *Membr. Water Treat.*, **6**(1), 27-42. <http://doi.org/10.12989/mwt.2015.6.1.027>.
- Kim, S.K., Shin, D.M. and Rhim, J.W. (2021), “Designing a high-efficiency hypochlorite ion generation system by combining cation exchange membrane aided electrolysis with chlorine gas recovery stream”, *J. Membr. Sci.*, **630**, 119318. <https://doi.org/10.1016/j.memsci.2021.119318>.
- Ko, J., Kim, S.K., Yoon, Y., Cho, K.H., Song, W., Kim, T.H., Myung, S., Lee, S.S., Hwang, Y.K., Kim, S.W. and An, K.S.

- (2018), "Eco-friendly cellulose based solid electrolyte with high performance and enhanced low humidity performance by hybridizing with aluminum fumarate MOF", *Mater. Today Energy*, **9**, 11-18. <https://doi.org/10.1016/j.mtener.2018.04.007>
- Lantagne, D.S. (2008), "Sodium hypochlorite dosage for household and emergency water treatment", *J. Am. Water Works Assoc.*, **100**, 106-119. <https://doi.org/10.2166/wh.2017.012>.
- Lee, J., Cha, H.Y., Min, K.J., Cho, J. and Park, K.Y. (2018), "Electrochemical nitrate reduction using a cell divided by ion-exchange membrane", *Membr. Water Treat.*, **9**(3), 189-194. <http://doi.org/10.12989/mwt.2018.9.3.189>.
- Levanov, A.V. and Isaikina, O.Y. (2020), "Mechanism and kinetic model of chlorate and perchlorate formation during ozonation of aqueous chloride solutions", *Ind. Eng. Chem. Res.*, **59**, 14278-14287. <https://doi.org/10.1021/acs.iecr.0c02770>.
- Lu, M.C., Chen, P.L., Huang, D.J., Liang, C.K., Hsu, C.S. and Liu, W.T. (2021), "Disinfection efficiency of hospital infectious disease wards with chlorine dioxide and hypochlorous acid", *Aerobiologia*, **37**, 29-38. <https://doi.org/10.1007/s10453-020-09670-8>.
- Mara, D. and Horan, N. (2003), *Handbook of Water and Wastewater Microbiology*, Academic Press, London, U.K.
- Palaty, Z. and Bendova, H. (2010), "Permeability of anion-exchange membrane for Cl<sup>-</sup> ions. Dialysis of hypochlorite acid in the presence of nickel chloride", *Membr. Water Treat.*, **1**(1), 39-47. <http://doi.org/10.12989/mwt.2010.1.1.039>.
- Piskin, B. and Turkun, M. (1995), "Stability of various sodium hypochlorite solutions", *J. Endod.*, **21**, 253-255. [https://doi.org/10.1016/S0099-2399\(06\)80991-X](https://doi.org/10.1016/S0099-2399(06)80991-X).
- Ryu, S., Kim, J.H., Lee, J.Y. and Moon, S.H. (2018), "Investigation of the effects of electric fields on the nano-structure of nafion and its proton conductivity", *J. Mater. Chem. A*, **6**, 20836-20843. <https://doi.org/10.1039/C8TA06752J>.
- Sanchez-Aldana, D., Ortega-Corral, N., Rocha-Gutierrez, B.A., Ballinas-Casarrubias, L., Perez-Dominguez, E.J., Nevarez-Moorillon, G.V., Soto-Salcido, L.A., Ortega-Hernandez, S., Cardenas-Felix, G. and Gonzalez-Sanchez, G. (2018), "Hypochlorite generation from a water softener spent brine", *Water* **10**, 1733. <https://doi.org/10.3390/w10121733>.
- Severing, A.L., Rembe, J.D., Koester, V. and Stuermer, E.K. (2019), "Safety and efficacy profiles of different commercial sodium hypochlorite/hypochlorous acid solutions (NaClO/HClO): Antimicrobial efficacy, cytotoxic impact and physico-chemical parameters in vitro", *J. Antimicrob. Chemother.*, **74**, 365-372. <https://doi.org/10.1093/jac/dky432>.
- Sone, Y., Ekdunge, P. and Simonsson, D. (1996), "Proton conductivity of Nafion 117 measured by a four-electrode ac impedance method", *J. Electrochem. Soc.*, **143**, 1254. <https://doi.org/10.1149/1.1836625>.
- Twort, A.C., Ratnayaka, D.D. and Brandt, M.J. (2000) *Water Supply*, Butterworth-Heinemann, Oxford, U.K.
- Urban, P. G. (2007) *Bretherick's Handbook of Reactive Chemical Hazards*, Academic Press, Oxford, U.K.
- Vijayaraghavan, K., Ahmad, D. and Yazid, A.Y.A. (2008), "Electrolytic treatment of latex wastewater." *Desalination*, **219**, 214-221. <https://doi.org/10.1016/j.desal.2007.05.014>.
- Vijayaraghavan, K., Ramanujam, T.K. and Balasubramanian, N. (1999), "In situ hypochlorous acid generation for the treatment of distillery spentwash", *Ind. Eng. Chem. Res.*, **38**, 2264-2267. <https://doi.org/10.1021/ie980166x>.
- Wang, Y., Xue, Y. and Zhang, C. (2020), "Generation and application of reactive chlorine species by electrochemical process combined with UV irradiation: synergistic mechanism for enhanced degradation performance", *Sci. Total Environ.*, **712**, 136501. <https://doi.org/10.1016/j.scitotenv.2020.136501>.
- Wilhelm, N., Kaufmann, A., Blanton, E. and Lantagne, D. (2018), "Sodium hypochlorite dosage for household and emergency water treatment: updated recommendations", *J. Water Health*, **16**, 112-125. <https://doi.org/10.2166/wh.2017.012>.
- Wilson, V.A. (1935), "Determination of available chlorine in hypochlorite solutions by direct titration with sodium thiosulfate", *Ind. Eng. Chem. Anal. Ed.*, **7**, 44-45. <https://doi.org/10.1021/ac50093a022>.
- Zierof, M.L., Polycarou, M.M. and Uber, J.G. (1998), "Development and autocalibration of an input-output model of chlorine transport in drinking water distribution systems", *IEEE T. Contr. Syst. T.*, **6**, 543-553. <https://doi.org/10.1109/87.701351>.

CC